Action Potentials - Hodgkin and Huxley Equation, Fitzhugh-Nagumo Equation

October 7, 2013

Hodgkin and Huxley Experiment

At a time when the mechanisms behind action potentials were debated between competing theories, Alan Hodgkin and Andrew Huxley carried out experiments which confirmed the ion channel model of action potentials. The key component of the experiment was the giant squid axon which can be up to 1 mm in diameter, very large for a neuron. The large girth of the squid axon facilitated measurements of action potentials because the equipment did not need to be as finely crafted. The technique employed by Hodgkin and Huxley is referred to as voltage clamping [3]. The figure below shows a layout which is fairly similar to the setup used in the experiment.

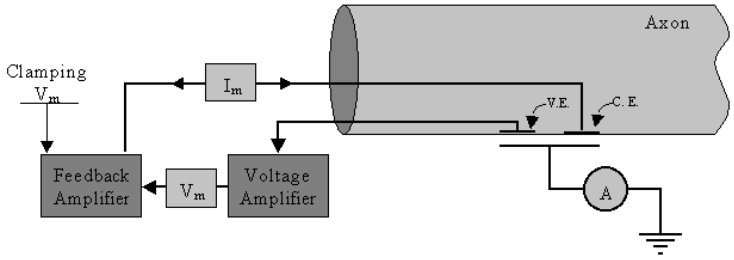

Figure 1: A diagram of the essential electrical components used in the patch-clamp method for measuring action potentials. Two electrodes (silver wires) are inserted axially into the axon. Then, a voltage amplifier and feedback amplifier are used to create and maintain a constant voltage while the current is measured via the second electrode.

The setup facilitated accurate measurements of membrane currents. Each of the two electrodes, which were inserted along the axis of the axon, were insulated except a region centered around the external electrodes. One of the internal electrodes was set up measure internal voltage changes and the other internal current changes of the axon. The system is driven by an external square-wave potential feed which is maintained as constant via a feedback amplifier. Constant potential minimizes any contribution the capacity current makes to the

measured total current [5]. The current can be measured easily with this setup, but experimental parameters must be altered to delve into the nature of the current.

Hodgkin-Huxley Model

Components

The action potential measured by Hodgkin and Huxley displayed an odd behavior. From the resting potential, the voltage rose quickly, fell slowly, overshot rest potential, and gradually rose back to equilibrium. The fact that the action potential overshot rest potential convinced the researchers that more than one single current was active in the axon. The external concentrations of Na^+ were lowered, and the resulting action potentials showed smaller magnitudes for the initial voltage spike for decreased Na^+ concentrations. The other prominent current was deduced to be K^+. Separate currents showed strong support for the ion channel model of action potentials. The results given in their experiments gave Hodgkin and Huxley reason to consider multiple components in their model. The strong initial spike in the action potential necessitated a Na^+ current component. The slow recovery response showed need for a K^+ component. Another leakage current which had no theoretical foundation was also evidenced in the data, so it was included as a component in the overall model.

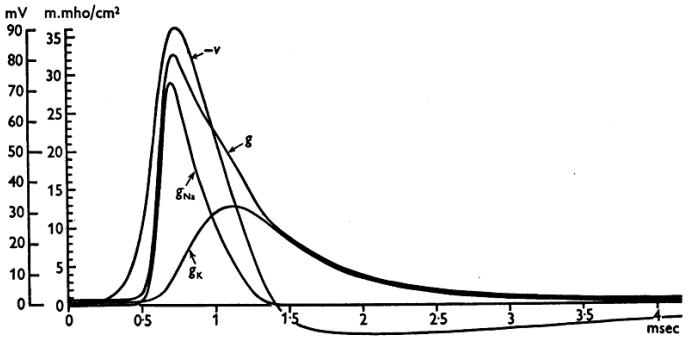

Figure 2: A graph from Hodgkin and Huxley's original paper [4] which contains four different labeled quantities: the membrane voltage, membrane conductance, Na^+ ion channel conductance, and K^+ ion channel conductance. The data spans a single squid action potential.

Formulation

Using all the data resulting from the patch-clamp experiment, Hodgkin and Huxley created a heuristic model through which action potential can be accurately reconstructed. The general formulation for the model is in terms of

electrical current via

$$I = gV. \tag{1}$$

The same basic equation retailored to incorporate multiple component currents and the chemical potential of each ion across the membrane is

$$I_k = g_k(V - V_k). \tag{2}$$

One essential element for modeling the excitable membrane potential is to consider the voltage-dependent of ions conductance. Rather than representing the conductance as a single fitted equation from experimental data, Hodgkin and Huxley postulated a set of membrane potential-influenced gating charges that control the conductance. To each gating charge corresponds a variable n_i. The conductance can then be expressed as

$$g_k = p_k(\{n_i\})\bar{g}_k \tag{3}$$

where $\bar{g}_k$ is the maximum conductance and $p_k(\{n_i\})$ is the fraction of the maximum conductance that the instantaneous conductance fulfills.

Each gating charge is assumed to behave independently of one another. Each gating charge also participates in first-order transitions between two states, labeled 'permissive' and 'non-permissive'. We will first examine the behavior of a single gating charge. For a first-order reaction, one has the following differential

$$\frac{dn}{dt} = \alpha_n(1 - n) - \beta_n n \tag{4}$$

in which α_n and β_n are the forward and backward rate constants respectively, and n is the probability of the gating charge being in the 'permissive' state. Alternatively using the voltage dependent time constant, $\tau_n = \frac{1}{\alpha_n+\beta_n}$, and the steady-state gating variable $n_\infty = \frac{\alpha_n}{\alpha_n+\beta_n}$ the differential equation becomes

$$\frac{dn}{dt} = \frac{n_\infty - n}{\tau_n}. \tag{5}$$

This differential equation has a solution which is a simple exponential.

$$n(t) = n_\infty - (n_\infty - n_0)\exp(-t/\tau_n) \tag{6}$$

Now if we assume that there are P gating charges for the given current, and that maximum conductance corresponds to every gating charge simultaneously being in the 'permissive' state, then we can interpret $p_k(\{n_i\})$ as the probability that every gating charge is in the 'permissive' state. i.e.

$$p_k(\{n_i\}) = \Pi_{i=1}^{P} n_i \tag{7}$$

The solution gives a strong foundation for fitting the gating variables to the

data, in particular the value of P. Now, incorporating the gating variables with equation 2 and empirical data [5], the final formulation for the Hodgkin-Huxley Equation is

$$I_{total} = n^4 \bar{g}_K (V - V_K) + m^3 h \bar{g}_{Na} (V - V_{Na}) + \bar{g}_L (V - V_L). \tag{8}$$

One finds that the K^+ current is controlled by 4 identical gating charges, whereas the Na^+ current is controlled by 3 identical and 1 distinct gating charge. The leak current, labeled by subscript L, is not voltage-dependent, and hence does not have any gating variables associated with its conductance.

Physical Interpretation of the Gating Variables

In fact, it is the gating charges lie in ion channels that control ion currents through the membrane. When ion channels open, ions diffuse through them down the concentration gradient across the membrane, giving rise to ion currents. There are different types of ion channels on the membrane, each selective for a different type*s* of ion.

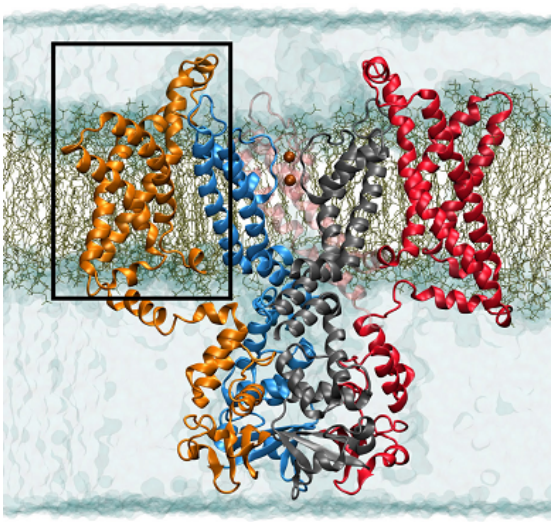

Figure 3: A VMD figure showing two of the four tetramers which constitute the Kv1.2 ion channel embeded in a lipid bilayer from Fatemeh Khalili's Thesis [6]. The box marker is indicative of the voltage sensing domain of the left monomer.

The conductivity for a particular current is then proportional to the fraction of channels that are open. But this fraction is equivalent to the probability of finding a given channel in the open state, namely $p_k(\{n_i\})$.

What about the gating charges? In each channel lie several charged residues that respond to changes in the membrane potential. These charged residues

constitute the gating charges of the channel.

We consider, for example, the voltage-gated potassium channel Kv1.2. This channel is a homotetramer. Each monomer contains a number of charged residues that make up the gating charge. In particular, the dominant contribution comes from four Arg residues in the transmembrane region. [8][1] When the gating charge switches between the 'permissive' and 'non-permissive' states, the positional change of the charged residues is equivalent to the movement of between 12 to 14 elementary charges across the transmembrane potential gradient. [7][8]

As one would expect from the fact that the four monomers are identical, the gating variable for this potassium channel is n^4.

Fitzhugh-Nagumo Model

The Hodgkin-Huxley Model proved to be very accurate and useful in further research into action potentials. However, the formula was rather complicated and relied heavily on empirical equations fit from data. A simpler formulation was needed to analyze such systems with mathematical rigor. Richard Fitzhugh rose to the task and helped formulate an approximation of the Hodgkin-Huxley Model which is now known as the Fitzhugh-Nagumo (FN) Model.

Derivation

The FN Model does not arrive directly from simplification of the HH Model, but the first step in arriving at the FN Model is simplifying the HH Model. Fitzhugh took the 4-dimensional HH Model and used approximate projections to cast it into an approximate 2-dimensional manifold of the original system [2]. One dimension contained both n and h. While the V and m variables are accounted in a second projection. The approximated 2-dimensional manifold of the HH Model shows strong similarity to a system with which Richard Fitzhugh was familiar, namely the Van der Pol oscillator. He defined what is now known as the FN Model by adding terms to a special case of the Van der Pol oscillator.

Formulation

The FN Model as a complete system is

$$\dot{x} = c(y + x - x^3/3 + z) = F_1(x, y) \tag{9}$$

$$\dot{y} = -(x - a + by)/c = F_2(x, y) \tag{10}$$

in which $a = 0.7$, $b = 0.8$, $c = 3$ are constant , and $z = -0.4$, which represents external excitation, for the standard representation.

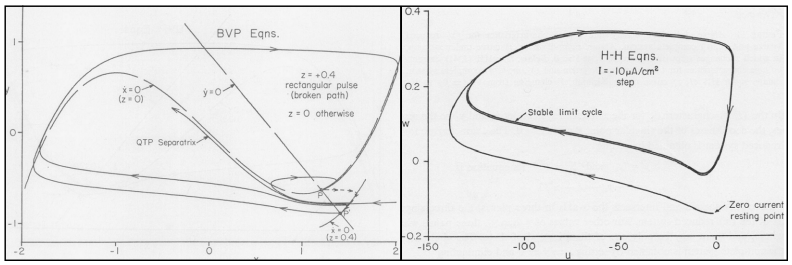

Figure 4: Two phase portraits which were included in one of Fitzhugh's original papers developing the FN Model. The limit cycle carved out by the FN Model is shown on the left and the limit cycle carved out by the 2-dimensional projection of the HH Model is shown on the right.

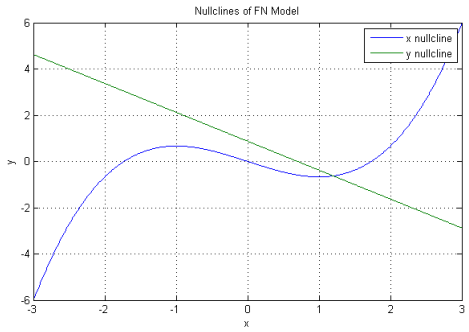

Figure 5: The graph includes both nullclines of the FN Model. The nullclines intersect at a singular point as shown clearly in the figure.

Mathematical Analysis

In order to develop better understanding the FN Model, analyzing the nullclines of the system is a good starting point. Nullclines are defined as lines on which a differential is zero in the phase plane. For the FN Model then, one arrives at

$$y = x^3/3 - x - z \tag{11}$$

$$y = (a - x)/b \tag{12}$$

which are shown below.
As the graph depicting the nullclines clearly displays, the system has a singular stationary point, $x_s \approx 1.19, y_s \approx 0.59$. In order to analyze the stability of this stationary point, let $x = x_s + \delta x$, $y = y_s + \delta y$ and take the first-order terms from a Taylor expansion around the stationary point.

$$\begin{bmatrix} \dot{\delta x} \\ \dot{\delta y} \end{bmatrix} = \begin{bmatrix} \frac{\partial F_1}{\partial x} & \frac{\partial F_2}{\partial y} \\ \frac{\partial F_1}{\partial x} & \frac{\partial F_2}{\partial y} \end{bmatrix} \begin{bmatrix} \delta x \\ \delta y \end{bmatrix} \tag{13}$$

The coefficient matrix of Taylor expansion terms can be easily evaluated.

$$M = \begin{bmatrix} (1-x^2)c & c \\ -1/c & -b/c \end{bmatrix} \tag{14}$$

In order to determine the stability of the stationary point, the eigenvalues of the matrix need to be resolved. Using standard methods the eigenvalues can be solved.

$$\lambda = \frac{\left[(1-x^2)c - b/c\right] \pm \sqrt{\left[(1-x^2)c - b/c\right]^2 - 4(1-b(1-x^2))}}{2} \tag{15}$$

Geometrically, we are looking at the dynamic of the system in the basis of its eigenvectors. By simple calculus, the solution of the system, with eigenvectors $\vec{v_1}$and $\vec{v_2}$, can be written as

$$\begin{bmatrix} \delta x \\ \delta y \end{bmatrix} = c_1 \vec{v_1} e^{\lambda_1 t} + c_2 \vec{v_2} e^{\lambda_2 t} \tag{16}$$

Hence, for stability, the real parts of the both eigenvalues should be less than zero so that the system will return to the stationary point upon small perturbation. Assuming a stable point is the end goal, two conditions follow from the eigenvalues defined above.

$$(1-x^2)c - b/c < 0 \tag{17}$$

$$1 - b(1-x^2) > 0 \tag{18}$$

In the standard FN Model, $b = 0.8$, which guarantees that (18) will always be true. The real boundary is then imposed by (17). The stability of the critical point depends on the value of x_s which in turn depends on z. As it happens $z = -0.4$ renders the stationary point unstable and induces limit cycles in the system. However, if $z > -0.34$ then the system contains a stable, stationary point. The stationary point of the system has been determined to

be unstable, so the system is unlikely to come to rest on that point. The rest of the differential system carves out a stable limit cycle in phase space. The limit cycle depicted in figure 4 can be understood intuitively when compared to the nullclines in figure 5. Observe that each differential component will change signs when crossing its respective nullcline and consider that, generally, the $\dot{x}$ component is larger in magnitude than the $\dot{y}$ component. In the FN Model,

the x variable is representative of the voltage across the membrane. If the most intuitive connection between the FN Model and HH Model is desired, one needs only to observe a plot of the voltage variable against time. Two cases should be considered, and are shown below. The first case is a single excitory voltage spike in the FN system with a stable stationary point, i.e. $z = 0$. The second case is a train of voltage impulses give by limit cycle behavior presented when $z = -0.4$.

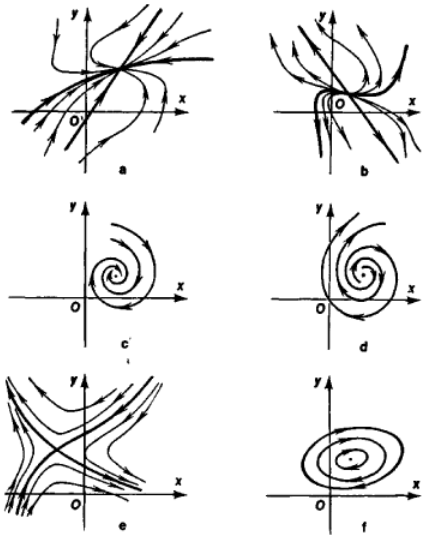

Figure 6: Phase trajectories in the neighborhood of the following types of singular points: (a) a stable node, (b) an unstable node, (c) a stable focus, (d) an unstable focus, (e) a saddle point, (f) a center for limit cycle

Both cases show strong similarity to the action potential give computations with the HH Model.

Linear stability analysis

The followings are all possible cases for the dynamics around a stationary point in 2-D. The nature of the stationary point is determined by the value of eigenvalues evaluated at the point, as shown in *figure* 6:
Forλ's are real,
i) $\lambda_1,\ \lambda_2 < 0$: stable node
ii) $\lambda_1 > 0,\ \lambda_2 < 0$ or vice versa: saddle node
iii) $\lambda_1,\ \lambda_2 > 0$: unstable node
For λ is a pair of complex conjugate,
i) $Re(\lambda_1),\ Re(\lambda_2) < 0$, stable focus
ii) $Re(\lambda_1),\ Re(\lambda_2) < 0$, unstable focus

Numerical solution

There is usually no analytic solution for nonlinear system like Fitzhugh-Nagumo model. One can apply the technique of numerical solution for those system. The simplest method is the Euler's method. Discretizing time into small interval gives $\frac{\vec{x}(t+\Delta t)-\vec{x}(t)}{\Delta t} \approx \vec{F}[\vec{x}(t)]$, hence one can solve forwards in time for the

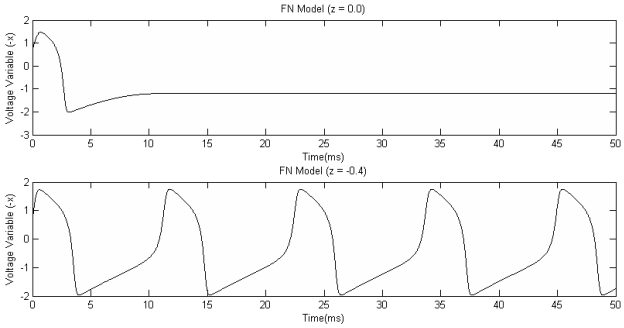

Figure 7: Action potentials simulated using the FN Model. The top figure represents are short-lived stimulus in the system producing a single action potential. The bottom figure corresponds to the system under a maintained external stimulus yielding a continuous train of impulses.

numerical solution for the dynamical system. For eq. (9) and (10),

$$\begin{aligned} x(t+\Delta t) &= x(t) + c(y(t) + x(t) - x^3/3 + z)\Delta t \\ y(t+\Delta t) &= y(t) - (x(t) - a + by(t))\Delta t/c \end{aligned} \tag{19}$$

This method has a global error of order Δt, which means reducing Δt by half will reduce the error in the solution by half.

Singular lines

Following the discussion in [9], one can understand the global dynamics of nonlinear system like Fitzhugh-Nagumo equation by looking at 'singular lines' on the phase plane. Define the lines with slope $m = \frac{F_2(x,y)}{F_1(x,y)}$, solving it yields $y = I(m,x)$. The condition for a line to be local attractors (all neighboring flows converge) or local separatrices is $\frac{\partial}{\partial x} I(m,x) = m$. In other words, on a 'singular line' the direction of force field coincides with the slope of the line. By implicit function theorem, one can write

$$m = -\frac{\frac{\partial}{\partial x}(F_2/F_1)}{\frac{\partial}{\partial y}(F_2/F_1)} = -\frac{\frac{\partial F_2}{\partial x} - m\frac{\partial F_1}{\partial x}}{\frac{\partial F_2}{\partial y} - m\frac{\partial F_1}{\partial y}} \tag{20}$$

this results in a quadratic equation in m

$$m^2 \frac{\partial F_1}{\partial y} + m\left(\frac{\partial F_1}{\partial x} - \frac{\partial F_2}{\partial y}\right) - \frac{\partial F_2}{\partial x} = 0 \tag{21}$$

So there can be two solutions $m_{1,2}(x,y)$ which corresponds to 'singular lines'. In order for the lines with slope $m_{1,2}(x,y)$ indeed correspond to 'singular lines', the consistency condition must be matched

$$\frac{\partial I}{\partial m}\frac{\partial m}{\partial x} = 0\,, \tag{22}$$

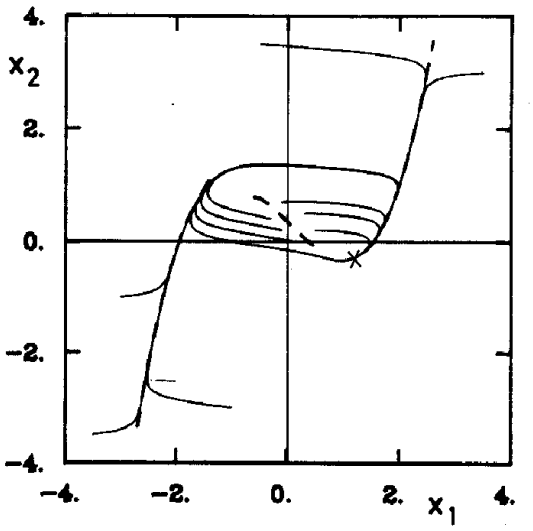

Figure 8: 'Singular lines' in Fitzhugh-Nagumo equation. The left and right parts of the x-nullcline serve as local attractors while the central part is a local separatrix, as indicated by the neighboring trajectories. Figure credit [9]

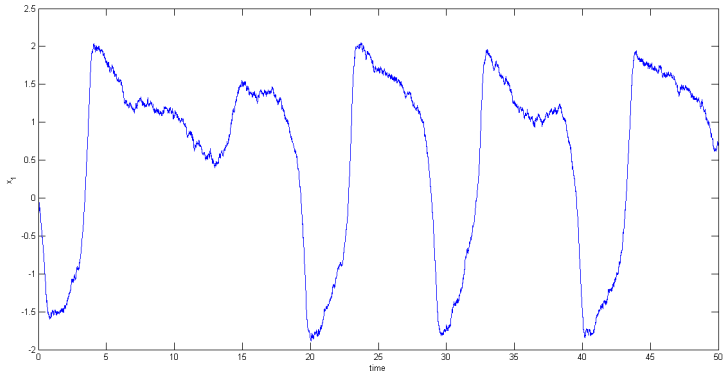

Figure 9: Noisy Fitzhugh-Nagumo equation. Once the system crosses the separatrix, a large negative response is initiated, corresponding to the thresholding behavior in neurons.

see [9] for more details. The resulting 'singular lines' are shown in *figure* 8. This geometrical feature allows the system to capture the thresholding behavior of neurons. For instance, when z=0, the stationary point is $(x, y) \approx (1.199, -0.624)$, represented by the cross in *figure* 8. Now consider a noisy system $\dot{\vec{x}} = \vec{F}(\vec{x}) + \sigma\vec{\xi}$, where $\vec{\xi}$ is white Gaussian noise, and σ is the amplitude of the noise. The case for $\sigma = 1$ is shown in *figure 9,* once noise drives the system across the separatrix, a large detour is initiated.

References

[1] S. K. Aggarwal and R. MacKinnon, *Contribution of the s4 segment to gating charge in the* Shaker k^+ *channel*, Neuron **16** (1996), 1169–1177.

[2] Richard Fitzhugh, *Impulses and physiological states in theoretical models of nerve membrane*, Biophysical Journal **1** (1961).

[3] Bertil Hille, *Ion channels of excitable membranes*, Sinauer, Sunderland, MA, 2001.

[4] A. L. Hodgkin and A. F. Huxley, *A quantitative description of membrane current and its application to conduction and excitation in nerve*, Journal of Physiology.

[5] A. L. Hodgkin, A. F. Huxley, and B. Katz, *Measurement of current-voltage relations in the membrane of the giant axon of loligo*, Journal of Physiology **116** (1952), 424,448.

[6] Fatemeh Khalili-Araghi, *Voltage-gating mechanism in potassium channels*, (2010).

[7] ... F.J. Sigworth N. E. Schoppa, K. McCormack, *The size of gating charge in wild-type and mutant* Shaker *potassium channels*, Science **255** (1992), 1712–1715.

[8] ... F. Bezanilla S. A. Seoh, D. Sigg, *Voltage-sensing residues in the s2 and s4 segments of the* Shaker k^+ *channel*, Neuron **16** (1996), 1159–1167.

[9] Herbert Treutlein and Klaus Schulten, *Noise induced limit cycles of the bonhoeffer-van der pol model of neural pulses*, Ber. Bunsenges. Phys. Chem **89** (1985), 710,718.